Multigrid Convergence for Convection-Diffusion Problems on Composite Grids

James S. Otto*
Department of Mathematics
University of Colorado at Denver
Denver, Colorado 80204

Submitted by Hans Schneider

ABSTRACT

We study the convergence behavior of the FAC (fast adaptive composite) multigrid method as applied to the solution of convection-diffusion equations discretized on composite grids in one and two dimensions. Analysis of the one-dimensional problem leads to the interpretation of two-level FAC as a direct solver. This analysis also provides important insight into the behavior of the method for the two-dimensional problem that has its flow velocity oriented in a single coordinate direction. For the latter problem we consider the use of standard upwind differencing on the coarse component of the grid, and allow the discretization type to vary on the fine component. When centered differencing is used on this fine region, we show that the behavior is very similar to that predicted by the analysis in one dimension. With a higher-order upwinding scheme used on this component, we show how to modify the discretization at the coarse-grid level in order to preserve the attractive convergence behavior predicted by the analysis.

1. INTRODUCTION

In this paper we study the convergence behavior of a multigrid variant as applied to the numerical solution of convection-dominated convection-diffusion equations discretized by a finite-volume method [9, 14, 15]. We

*This work was supported in part by NSF Grant DMS 8704169 and DOE Grant DE-FG02-90ER25086.

655 Avenue of the Americas, New York, NY 10010 0024-3795/93/$6.00

consider solving one- and two-dimensional problems whose true solutions are such that the use of a significant level of local grid refinement on an otherwise (relatively) coarse grid is desirable. The particular algorithm we investigate is a two-level version of the FAC (fast adaptive composite) scheme [12], but our results also shed light on other closely related methods [2, 8, 16]. This material has been adopted from the study of that method in [14, Chapter 4]. Although this paper deals with the convergence behavior of two-level FAC, we are motivated by the work of Chin and Manteuffel in [6]. There, the authors consider the solution of the two-dimensional convection-diffusion equation

$$-\varepsilon\Delta u(\hat{x}, \hat{y}) + au_{\hat{x}}(\hat{x}, \hat{y}) + bu_{\hat{y}}(\hat{x}, \hat{y}) + du(\hat{x}, \hat{y}) = g(\hat{x}, \hat{y}), \quad (1.1)$$

where ε is a small positive constant. Notice that if ε is equal to zero in (1.1), then the equation is pure convection and is easily solved, in principle, by integrating along its characteristics. In practice, however, the characteristics may be difficult to track, and in any case we are interested in solving the problem with ε small but positive. Nevertheless, when ε is sufficiently small one feels that advantage may still be gained from the problem's nearly one-dimensional character. In [6] the authors do this by using an orthogonal coordinate transformation that is induced by the characteristics. Under appropriate assumptions, the latter transforms (1.1) into the equation

$$-\varepsilon\Delta u(x, y) + u_x(x, y) + cu(x, y) = f(x, y). \quad (1.2)$$

With this form, the characteristics are simply y = constant, and any procedure that employs solving along the characteristic directions (such as relaxation) will be facilitated by having the characteristics aligned with gridlines in a Cartesian-product grid. In [6] the authors analyze the spectrum of the block SOR iteration matrix associated with a centered-difference discretization of (1.2) (with $c = 0$). This iteration is based on alternative matrix splittings that use either the x- or y-derivative terms of the discretization as the principal part of the splitting. The relative size of the diffusion coefficient is measured by the ratio $\gamma = h/(2\varepsilon)$, where h is the meshsize. When the problem is convection dominated (i.e., for $\gamma \geqslant 1$), and with relaxation performed along lines in the x-direction, they obtain a bound on the spectral radius of the iteration matrix that is less than $\frac{1}{5}$.

We also consider the numerical solution of (1.2). One way that our strategy differs from [6] is in allowing multigrid to play the role of the iterative solver. The FAC algorithm discussed here may be implemented in such a way as to retain the essential parallelizability of the problem in the

above form by using block Jacobi, or line relaxation, as the smoother on which multigrid is based. In such an implementation, exact solutions of subgrid problems are replaced by inexpensive multigrid approximations. We use a finite-volume method for our composite-grid discretization of (1.2). On uniform subgrids, the resulting matrix stencils are familiar five-point difference ones that capture all of the convection of (1.2) in their main-diagonal blocks. Therefore, block Jacobi is particularly effective as an iterative solver and as a multigrid smoother for these subgrid problems, when ε is small (see [14, Chapter 5] for details). We note that the choice of a relaxation method does not play a role in this paper, since we assume the FAC algorithm to be carried out in its true two-level form, i.e., with exact solves of the subgrid problems performed. Our intent here is to demonstrate the effectiveness of the two-level scheme and to gain insight into its behavior for the various discretizations that might be used on the components of the composite grid, and on an underlying global coarse grid.

An overview of this paper follows. In Section 2, we introduce the composite grid structure. The use of this structure allows for immediate refinement of the grid in a region, or *patch*, where the solution changes rapidly. We emphasize the use of multiple levels of patch refinement in this study and investigate the effects that using such refinement has on FAC convergence. The composite grid structure also provides a convenient way of interfacing different discretization types on subregions of the grid. We consider the use of various discretizations (upwind, centered, and second-order upwind) on the patch component of the grid, along with the use of standard upwinding outside of the patch (i.e., on the grid's coarse component).

Section 3 begins with a description of two-level FAC. We also give an important characterization of the method as an interface preconditioning. Section 3.1 is an analysis of the convergence of the two-level scheme as applied to the one-dimensional convection-diffusion equation

$$\begin{aligned} -\varepsilon u''(x) + u'(x) &= f(x), \qquad x \in \Omega = [0,1], \\ u(0) &= 1, \qquad u'(1) = \alpha. \end{aligned} \tag{1.3}$$

Our analysis allows the finite-volume discretization to vary in type, from upwind to centered differences, on the patch component of the fine and coarse composite grids. We note that the results of this analysis are similar in character to the results in [1] and [11] for uniform grids.

Section 3.2 is an experimental study of FAC applied to the problem

$$\begin{aligned} -\varepsilon\Delta u(x,y) + u_x(x,y) &= f(x,y), \qquad (x,y) \in \Omega = [0,1] \times [0,1], \\ u(x,0) &= g_1(x), \\ u(0,y) &= g_2(y), \\ u_x(1,y) &= \alpha(y), \\ u(x,1) &= g_3(x). \end{aligned} \tag{1.4}$$

Taking a cue from the one-dimensional analysis, we use as the basis for these experiments a FAC method that employs a global coarse grid at the coarse level in the two-level scheme. The convergence behavior here is seen to conform generally to the analysis of Section 3.1. This is particularly true for a method that employs centered differencing on the fine patch and upwind differencing on the coarse-level grid. We show that convergence improves with increasing refinement on the patch. We also note that convergence factors obtained from the one-dimensional analysis provide reliable estimates of convergence rates for this method in two dimensions. This information may be used to design a strategy for switching discretization types when the FAC scheme is used in a nested way on a succession of composite grids.

On the other hand, when standard upwinding is used on the fine patch, it is discovered that the convergence rates deteriorate at the tangential boundaries of the patch. The reason for this degradation is demonstrated, and a successful remedy that involves modification of the coarse-grid stencil is implemented. Similar results are obtained for higher-order upwinding. These results indicate that the use of higher-order upwinding can replace standard upwinding on the fine patch with little sacrifice in efficiency. Generally, the results of this section indicate that the two-level scheme provides a good algebraic solver for the convection-dominated problem. This observation motivates the use of FAC in [14, Chapter 5].

There, FAC is employed as a weak algebraic solver on each of the composite grids in the succession of grids lying between the global coarse grid and the true composite grid. Computational results presented there show that, for the various discretization mixtures, only one or two FAC iterations are required on each of the composite levels to obtain an approximation by this version of FAC with accuracy comparable to the exact solution of the composite-grid equations. Furthermore, it is shown that this is the case with complete solves of problems on the subregions replaced by inexpensive approximations.

Section 4 is a summary of the results of this paper.

2. DESCRIPTION OF COMPOSITE GRIDS

This section describes the composite grids to be used in this paper. The structure we employ for the grids is that of [13]. This description applies to the case of a rectangular domain in two dimensions, and we suppose the subregion of the domain requiring refinement to be an interior region that does not intersect the boundary. Although no assumptions are made concerning the shape of this region, we will only consider refinement of the grid on a rectangular patch. Generalizations of these concepts to L-shaped grids and refinements, other dimensions, and refinements at corners and boundaries of the domain can easily be made, but for the purposes of this paper we restrict our attention to the above simple case. Although we only describe in detail the two-dimensional case, the structure of the composite grid in one dimension is very similar, and it should be straightforward for the reader to adapt the following definitions to the situation in one dimension.

Suppose we are given a rectangular h-grid with uniform spacing, h being the node-to-node distance in both the x- and y-directions. A composite grid is determined by choosing some rectangular subset of nodes along with a positive integer, m, indicating the *order of refinement*. The set of nodes forming the boundary of the subset is called the *interface*. We assume that each side of the interface has at least three nodes (including corners), so that the interior of the rectangular subset is nonempty. This set of interior nodes is called the *coarse patch*.

If we designate the set of nodes exterior to the interface as the *coarse* nodes, then we have the uniform h-grid as the union of three components: coarse, interface, and coarse patch. We call this grid the *global uniform coarse grid* or just *global coarse grid*. See Figure 1.

The *composite grid* is obtained from the global coarse grid by adding nodes to the coarse patch; the *fine patch* component of the composite grid is the set of interior nodes of the uniform h_F-grid on the region bounded by the interface, where $h_F = h/2^m$. The set of boundary nodes for the fine patch (which contains the interface) is called the *fine boundary*, but aside from the interface nodes it is not considered part of the composite grid. However, we define the complement of the interface in the fine boundary as an adjuvant to the composite grid called the set of *slave nodes*. Though not technically belonging to the composite grid, they play an essential role in the definition of the composite discretization [13, 14]. In summary, the composite grid is made up of three components, coarse and interface components being the same as for the global coarse grid, along with a fine component obtained via "refinement on the patch." An example of a composite grid (with one refinement) is shown in Figure 2.

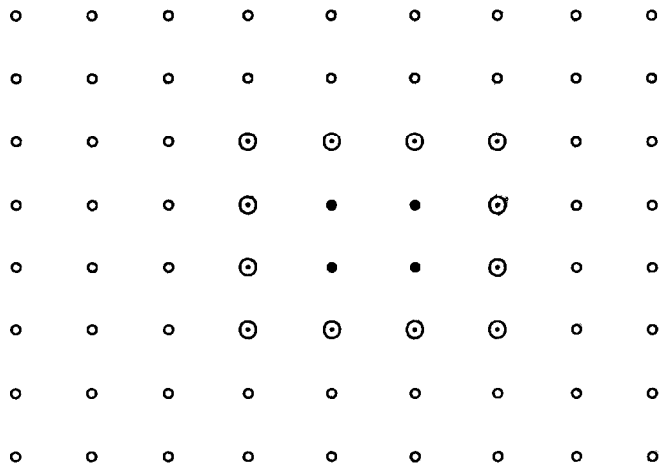

FIG. 1. Global coarse grid with coarse (○), fine (●), and interface (⊙) nodes.

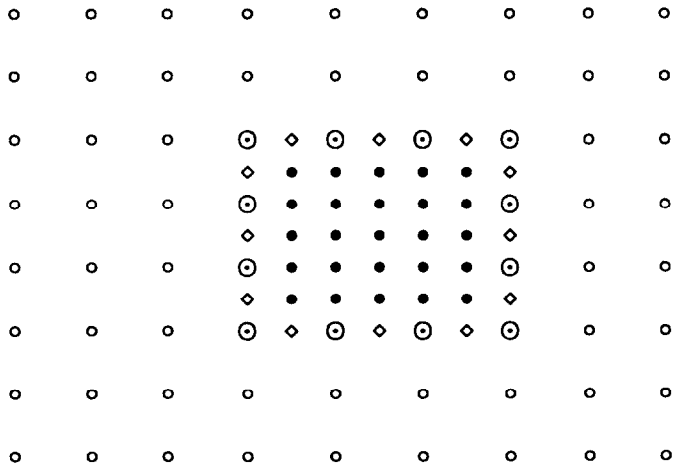

FIG. 2. Composite grid with coarse (○), fine (●), interface (⊙), and slave (◇) nodes.

3. CONVERGENCE OF FAC

This section studies the convergence of FAC as an iterative solver for convection-diffusion equations on the composite grids of Section 2.

We partition vectors in the composite grid space into three components: coarse, interface, and fine patch. As for notation, members of the composite grid space are represented by lowercase roman letters distinguished by an underscore, and components by the lowercase letters subscripted with C, F, or I. For example, a composite right-hand side (or residual) is written

$$\underline{\mathbf{r}} = [\mathbf{r}_C, \mathbf{r}_F, \mathbf{r}_I].$$

Similar notation is used for composite grid operators and their components. The composite grid equation $\underline{\underline{L}}\underline{\mathbf{z}} = \underline{\mathbf{r}}$ may then be written as

$$\begin{bmatrix} L_C & 0 & L_{CI} \\ 0 & L_F & L_{FI} \\ L_{IC} & L_{IF} & L_I \end{bmatrix} \begin{bmatrix} \mathbf{z}_C \\ \mathbf{z}_F \\ \mathbf{z}_I \end{bmatrix} = \begin{bmatrix} \mathbf{r}_C \\ \mathbf{r}_F \\ \mathbf{r}_I \end{bmatrix}. \tag{3.1}$$

A word of explanation with regard to the notation accompanying the components of $\underline{\underline{L}}$: in general, L_{XY} denotes that portion of the stencil of the matrix $\underline{\underline{L}}$ that represents the connections to nodes in component Y that appear in the equations for the nodes in component X, i.e., entries $\underline{\underline{l}}_{ij}$ where node i lies in X and node j lies in Y. Also, L_I, for example, stands for the interface-to-interface connections.

We begin by describing the method without regard to an underlying differential equation or discretization method. Then, in Sections 3.1 and 3.2, we consider the convergence behavior of the method as applied to finite-volume discretizations of Equations (1.3) and (1.4), respectively. In what follows, appropriate consistency of composite operators and their components as described in [7] is assumed.

FAC [12, 13] is an adaptation of multigrid to composite-grid problems and as such makes use of a coarse-grid discretization of the differential operator to obtain approximations to the fine-grid error left by relaxation. In the present context, one may think of the fine-grid operator as being the composite-grid operator defined above. As for the coarse-grid operator, it is useful in defining it to retain some flexibility. We accept in this role a discretization on any of the composite grids that lie between the global coarse grid and the true composite grid (the grid on which the discrete solution is ultimately sought). These grids are the ones obtained from the global coarse

grid in the same manner as the true composite grid, but differ by having less refinement on the patch (all grids agree in their coarse and interface components). An important special case to consider is the global coarse grid viewed as a composite grid. Since this grid is uniform, in principle no special considerations need apply in defining the operator, that is, a standard discretization based on a lexicographic ordering of the nodes and equations, for example, may be used. Also, since the grid is uniform, it is possible to apply any one of a variety of well-known, highly effective methods to solve standard problems on this grid.

The uniformity of the global coarse grid is its attractive feature. However, we retain the viewpoint put forth in Section 2 that it is itself a composite grid and that the discretization on it yields a composite-grid operator. It makes sense, then, to refer in general to the coarse grid as the *coarse composite* grid (the phrase *composite grid* may be reserved for the true composite grid when distinguishing the levels in the two-level algorithm). Once this viewpoint is taken, the strategy of using different discretizations on the coarse and patch components of the coarse grid becomes a possibility for all choices of this grid. We investigate in this section the effect of using various discretizations on the coarse grid, in terms of FAC convergence.

When denoting the grid operators, L is used as above in denoting the composite operator and its components, and A is used similarly for the coarse (composite) grid operator. Generally, notation developed for global coarse objects is used to refer to coarse composite ones. So, for example, the refinement region on the coarse composite grid is referred to as "the coarse patch."

Let $\underline{\boldsymbol{A}}$ be the discrete operator on this grid. Its component form is

$$\underline{\boldsymbol{A}} = \begin{bmatrix} A_C & 0 & A_{CI} \\ 0 & A_P & A_{PI} \\ A_{IC} & A_{IP} & A_I \end{bmatrix}.$$

Here, the subscript P refers to the coarse patch, as opposed to F, which refers to the fine-patch component of the (true) composite grid.

The following description of FAC corresponds to the delayed-correction version in its two-grid form as described in [13]. A subscript G is used to distinguish coarse composite vectors and components from true composite ones.

FAC ALGORITHM FOR THE SOLUTION OF $\underline{\boldsymbol{L}}\underline{\mathbf{z}} = \underline{\mathbf{r}}$. Let $\underline{\mathbf{z}}^0$ be given, and set $\underline{\mathbf{r}}^0 = \underline{\mathbf{r}} - \underline{\boldsymbol{L}}\underline{\mathbf{z}}^0$.

Loop on i: $i = 0, 1, \ldots,$ until convergence.

Step 1. Solve $\underline{\mathbf{A}}\mathbf{z}_G = \mathbf{r}_G = (\mathbf{r}_C^i, \mathbf{r}_P^i = I_F^P \mathbf{r}_F^i, \mathbf{r}_I^i)$ for

$$\mathbf{z}_G = (\mathbf{z}_{G,C}, \mathbf{z}_{G,P}, \mathbf{z}_{G,I}).$$

Step 2. Solve $L_F \mathbf{z}'_F = \mathbf{r}_F^i - L_{FI}\mathbf{z}_{G,I}$ for $\mathbf{z}'_F$.

Step 3. Perform the composite correction

$$\mathbf{z}_C^{i+1} = \mathbf{z}_C^i + \mathbf{z}_{G,C},$$

$$\mathbf{z}_F^{i+1} = \mathbf{z}_F^i + \mathbf{z}'_F,$$

$$\mathbf{z}_I^{i+1} = \mathbf{z}_I^i + \mathbf{z}_{G,I}.$$

Step 4. Set $\underline{\mathbf{z}}^{i+1} = (\mathbf{z}_C^{i+1}, \mathbf{z}_F^{i+1}, \mathbf{z}_I^{i+1})$, and form the new composite residual, $\underline{\mathbf{r}}^{i+1} = \underline{\mathbf{r}} - \underline{\boldsymbol{L}}\underline{\mathbf{z}}^{i+1}$.

End loop.

Here, I_F^P represents a restriction operator mapping the fine patch to the coarse patch.

Having defined the FAC algorithm, we now turn to a study of its convergence behavior. Assuming the exact solution of the global coarse- and fine-patch subproblems (i.e. exact inversion of $\underline{\mathbf{A}}$ and L_F) and assuming a natural coarse-component compatibility requirement, namely, $A_C = L_C$, $A_{CI} = L_{CI}$, and $A_{IC} = L_{IC}$, then [14, 10] for $i \geqslant 1$ we have $\mathbf{r}_C^i, \mathbf{r}_F^i = 0$ and

$$\mathbf{r}_I^i = \left(I_I - \hat{L}_I \hat{A}_I^{-1}\right)\mathbf{r}_I^{i-1}, \tag{3.2}$$

where

$$\hat{L}_I \equiv L_I - L_{IC}L_C^{-1}L_{CI} - L_{IF}L_F^{-1}L_{FI}$$

is the *Schur complement* in $\underline{\underline{L}}$ with respect to the partitioning (3.1), and

$$\hat{A}_I = A_I - L_{IC} L_C^{-1} L_{CI} - A_{IP} A_P^{-1} A_{PI}.$$

It is a distinguishing feature of FAC (and the closely related BEPS scheme [8, 10]) that it uses $\hat{A}_I$, the Schur complement with respect to the coarse-grid discretization, to precondition $\hat{L}_I$. Notice that the eigenvalues of $\hat{L}_I \hat{A}_I^{-1}$ are those values of λ for which the matrix

$$\hat{L}_I - \lambda \hat{A}_I = L_I - \lambda A_I + (\lambda - 1) L_{IC} L_C^{-1} L_{CI}$$

$$- L_{IF} L_F^{-1} L_{FI} + \lambda A_{IP} A_P^{-1} A_{PI}$$

is singular. This criterion for determining the eigenvalues will be applied in the next section.

3.1. Convergence in One Dimension

We now turn to an examination of the convergence of the FAC algorithm when it is applied to the solution of the finite-volume discretization of the problem (1.3). Since the operators $\underline{\underline{A}}$ and $\underline{\underline{L}}$ arising from this discretization satisfy the compatibility conditions, $A_C = L_C$, $A_{CI} = L_{CI}$, and $A_{IC} = L_{IC}$, it follows that convergence of the algorithm is governed by the relationship (3.2). We are therefore interested in the eigenvalues of the matrix $\hat{L}_I \hat{A}_I^{-1}$. Here, we assume that there is only one refinement region. An analysis for the case of multiple regions can be found in [14].

With a single refinement region on the one-dimensional composite grid, the operator $\underline{\underline{L}}$ of (3.1) has the structure shown in Figure 3. Notice that two nodes constitute the interface, so the dimensionality of the eigenvalue problem is equal to two. Therefore, identifying the required eigenvalues is "simply" a matter of the solving the quadratic equation

$$\mathrm{Det}\left(\hat{L}_I - \lambda \hat{A}_I\right) = 0$$

for λ. For the problem under consideration the analysis is facilitated by the fact that this quadratic appears, essentially, in factored form.

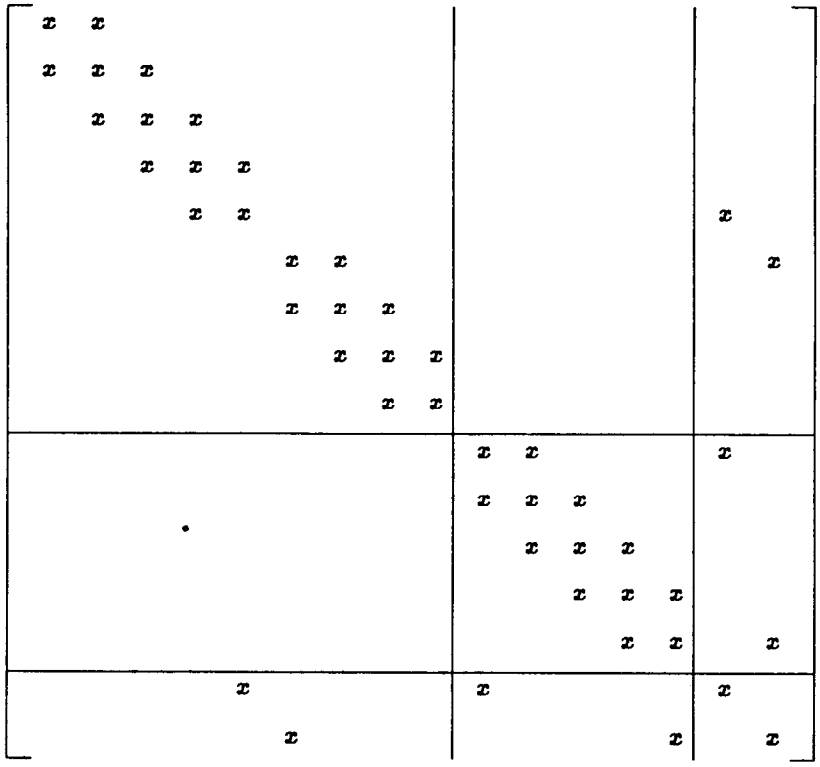

FIG. 3. Structure of a one-dimensional composite operator for the case of a single refinement region.

Denote the components of the composite operators as follows:

$$L_C = \begin{bmatrix} L & 0 \\ 0 & R \end{bmatrix}, \qquad L_{CI} = \begin{bmatrix} 0 & 0 \\ \vdots & \vdots \\ 0 & 0 \\ l_{CI} & 0 \\ 0 & r_{CI} \\ \vdots & \vdots \\ 0 & 0 \end{bmatrix},$$

$$L_{IC} = \begin{bmatrix} 0 & \cdots & 0 & l_{IC} & 0 & 0 & \cdots & 0 \\ 0 & \cdots & 0 & 0 & r_{IC} & 0 & \cdots & 0 \end{bmatrix},$$

$$L_I = \begin{bmatrix} l_I & 0 \\ 0 & r_I \end{bmatrix},$$

$$L_{FI} = \begin{bmatrix} l_{FI} & 0 \\ 0 & 0 \\ \vdots & \vdots \\ 0 & 0 \\ 0 & r_{FI} \end{bmatrix}, \qquad A_{PI} = \begin{bmatrix} l_{PI} & 0 \\ 0 & 0 \\ \vdots & \vdots \\ 0 & 0 \\ 0 & r_{PI} \end{bmatrix},$$

$$L_{IF} = \begin{bmatrix} l_{IF} & 0 & \cdots & 0 & 0 \\ 0 & 0 & \cdots & 0 & r_{IF} \end{bmatrix},$$

$$A_{IP} = \begin{bmatrix} l_{IP} & 0 & \cdots & 0 & 0 \\ 0 & 0 & \cdots & 0 & r_{IP} \end{bmatrix}.$$

We assume that the Dirichlet value at the left boundary has been moved to the right-hand side of (3.1). Let the respective orders of the matrices L, R, L_F, and A_P be N_{C_1}, N_{C_2}, N_F, and N_P. Also, let N_C be one less than the number of nodes on the global coarse grid (i.e., the order of the global coarse matrix with the left Dirichlet condition eliminated). The coarse meshwidth is denoted by $h = 1/N_C$. Denote the ijth element of X^{-1}, the inverse of the generic square invertible matrix X, by $\tilde{x}_{ij}$. Also, let $X_{j\times j}$ denote the $j \times j$ submatrix located in lower right corner of X. For example, if X is of order N, then $X_{1\times 1} = x_{NN}$ and $X_{N\times N} = X$. With this notation, we have

$$L_{IC} L_C^{-1} L_{CI} = \begin{bmatrix} l_{IC} l_{CI} \tilde{l}_{N_{C_1} N_{C_1}} & 0 \\ 0 & r_{IC} r_{CI} \tilde{r}_{11} \end{bmatrix},$$

$$L_{IF} L_F^{-1} L_{FI} = \begin{bmatrix} l_{IF} l_{FI} \tilde{l}_{F_{11}} & l_{IF} r_{FI} \tilde{l}_{F_{1,N_F}} \\ r_{IF} l_{FI} \tilde{l}_{F_{N_F,1}} & r_{IF} r_{FI} \tilde{l}_{FN_F,N_F} \end{bmatrix}, \tag{3.3}$$

$$A_{IP} A_P^{-1} A_{PI} = \begin{bmatrix} l_{IP} l_{PI} \tilde{a}_{P_{11}} & l_{IP} r_{PI} \tilde{a}_{P_{1,N_P}} \\ r_{IP} l_{PI} \tilde{a}_{P_{N_P,1}} & r_{IP} r_{PI} \tilde{a}_{P_{N_P,N_P}} \end{bmatrix}.$$

In order to continue, we need to obtain explicit representations for certain elements of the matrices L^{-1}, R^{-1}, L_F^{-1}, and A_P^{-1}. Notice that the above

formulas only involve the corner elements of these matrices. To denote our use of various finite-volume discretizations, we use a notation that indicates discretizations that change in type on the components of the coarse composite and true composite grids. We use a four-tuple, $(x_1, x_2 : x_3, x_4)$, with elements x_1 through x_4 that indicate the type of discretization used on the respective coarse component of the coarse composite grid, coarse patch, coarse component of the composite grid, and fine patch. The interface nodes are not specified here. In this section, the type of discretization at these points will always be of the same type used on the coarse component. (In two dimensions, it will be useful to allow more flexibility at the interface of the coarse composite grid.) In one dimension, two possibilities are considered: upwind ($x_i = U$) and centered ($x_i = C$) versions of the finite-volume discretization. In two dimensions, we will also allow higher-order upwinding to be used on the patch. In this paper, we limit our consideration to the case that upwinding is used on the coarse components of the grid, i.e., $x_1 = x_3 = U$. Generally, it will be possible to make the notation just described less cumbersome by employing obvious abbreviations. Initially, we will consider discretizations that agree in type throughout the two grids.

The first case we consider in detail is the discretization signified by $(U, U : U, U) = U^4$, which corresponds to upwinding used throughout the coarse composite and true composite grids. The analysis will make use of the generic tridiagonal matrix $X = \text{tri}[-\varepsilon - h, 2\varepsilon + h, -\varepsilon]$ of generic order N. Of interest are the corner elements of X^{-1}: $\tilde{x}_{11}$, $\tilde{x}_{1N}$, $\tilde{x}_{N1}$, and $\tilde{x}_{NN}$. Let X_{ij} be the cofactor of x_{ij}. The well-known formula

$$\tilde{x}_{ij} = X_{ji}/\text{Det } X$$

for the elements of the inverse serves as the basis for the following lemma.

LEMMA 3.1.1. *The four corner elements of X^{-1} corresponding to the upwind discretization are given by*

$$\tilde{x}_{11} = \tilde{x}_{NN} = \frac{z_{N-1}}{z_N} = \frac{(\varepsilon + h)^N - \varepsilon^N}{(\varepsilon + h)^{N+1} - \varepsilon^{N+1}} \approx \frac{1}{\varepsilon + h}, \tag{3.4}$$

$$\tilde{x}_{1N} = \frac{h \cdot \varepsilon^{N-1}}{(\varepsilon + h)^{N+1} - \varepsilon^{N+1}} \approx 0, \tag{3.5}$$

$$\tilde{x}_{N1} = \frac{h \cdot (\varepsilon + h)^{N-1}}{(\varepsilon + h)^{N+1} - \varepsilon^{N+1}} \approx \frac{h}{(\varepsilon + h)^2}. \tag{3.6}$$

Proof. Since X is tridiagonal, there is a three-term linear homogeneous difference equation for the jth determinant, $z_j \equiv \text{Det } X_{j\times j}$:

$$z_j = (2\varepsilon + h)z_{j-1} - \varepsilon(\varepsilon + h)z_{j-2}, \qquad j = 3, 4, \ldots, N.$$

The associated characteristic equation is

$$\mu^2 - \mu(2\varepsilon + h) + \varepsilon(\varepsilon + h) = 0,$$

with roots

$$\mu_1 = \varepsilon + h, \qquad \mu_2 = \varepsilon.$$

Hence, it follows from the theory of difference equations that

$$z_j = S(\varepsilon + h)^j + T\varepsilon^j,$$

where S and T are unknown constants which are determined uniquely by the values of z_1 and z_2. But

$$z_1 = S(\varepsilon + h) + T\varepsilon = 2\varepsilon + h,$$

$$z_2 = S(\varepsilon + h)^2 + T\varepsilon^2 = 3\varepsilon^2 + 3\varepsilon h + h^2.$$

Thus,

$$S = \frac{\varepsilon + h}{h}, \qquad T = -\frac{\varepsilon}{h},$$

and we have

$$z_j = \frac{(\varepsilon + h)^{j+1}}{h} - \frac{\varepsilon^{j+1}}{h}.$$

Now since X is tridiagonal, it follows that the cofactors satisfy

$$X_{11} = X_{NN} = \text{Det } X_{N-1\times N-1}.$$

Thus,

$$\tilde{x}_{11} = \tilde{x}_{NN} = \frac{z_{N-1}}{z_N} = \frac{(\varepsilon + h)^N - \varepsilon^N}{(\varepsilon + h)^{N+1} - \varepsilon^{N+1}}.$$

Also, $X_{N1} = \varepsilon^{N-1}$ implies that

$$\tilde{x}_{1N} = \frac{h \cdot \varepsilon^{N-1}}{(\varepsilon + h)^{N+1} - \varepsilon^{N+1}}.$$

Finally, $X_{1N} = (\varepsilon + h)^{N-1}$ implies that

$$\tilde{x}_{N1} = \frac{h \cdot (\varepsilon + h)^{N-1}}{(\varepsilon + h)^{N+1} - \varepsilon^{N+1}}. \qquad \blacksquare$$

More will be said shortly regarding the quality of the approximations given in the lemma (see the comments below and also the next section), but because of the last two approximations we will see that $\hat{L}$ and $\hat{A}$ are essentially lower triangular, so $\mathrm{Det}(\hat{L}_I - \lambda \hat{A}_I)$ just depends on the diagonal part of the matrix.

We may let X here assume the role of A_P when the coarse patch has trivial refinement, i.e., when the global coarse grid plays the role of the coarse composite grid in the two-level version of FAC. We have just found the required elements of the inverse of this operator. In this context, it may be useful to point out an apparent ambiguity in the above expressions. Notice that in these expressions, h is always directly related to the dimension, N_C, of the global coarse grid. However, the role of N in the expressions is allowed to vary. For example, when the approximations are made with regard to A_P, then $N \leftarrow N_P$ in (3.4)–(3.6), and note that, necessarily, $N_P < N_C$. One sees that there is an interplay between the size of ε and the dimensions of the global coarse and coarse-patch grids that enters into the validity of the approximations. In this particular case, their validity is commensurate with ε being small with respect to h (the reciprocal of N_C) and the coarse patch being sufficiently large.

Also, X may play the role of the coarse-component operators L and R, so that

$$\tilde{l}_{N_{C_1}, N_{C_1}} \tilde{r}_{11} \approx \frac{1}{\varepsilon + h}.$$

Now suppose that there are m levels of refinement on the fine patch. Then

$$L_F = 2^m \operatorname{tri}\left[-\varepsilon - \frac{h}{2^m}, 2\varepsilon + \frac{h}{2^m}, -\varepsilon\right],$$

and

$$\operatorname{Det} L_F = (2^m)^{N_F} \frac{(\varepsilon + h/2^m)^{N_F+1} - \varepsilon^{N_F+1}}{h/2^m}.$$

Using these expressions, we obtain the following corollary to Lemma 3.1.1.

COROLLARY 3.1.2. *The corner elements of the fine-patch matrix L_F corresponding to the upwind discretization are given by*

$$\tilde{l}_{F_{11}} = \tilde{l}_{F_{N_F,N_F}} = \frac{(\varepsilon + h/2^m)^{N_F} - \varepsilon^{N_F}}{2^m\left[(\varepsilon + h/2^m)^{N_F+1} - \varepsilon^{N_F+1}\right]} \approx \frac{1}{2^m\varepsilon + h}, \quad (3.7)$$

$$\tilde{l}_{F_{1,N_F}} = \frac{h \cdot \varepsilon^{N_F-1}}{2^{2m}\left[(\varepsilon + h/2^m)^{N_F+1} - \varepsilon^{N_F+1}\right]} \approx 0, \quad (3.8)$$

$$\tilde{l}_{F_{N_F,1}} = \frac{h \cdot (\varepsilon + h/2^m)^{N_F-1}}{2^{2m}\left[(\varepsilon + h/2^m)^{N_F+1} - \varepsilon^{N_F+1}\right]} \approx \frac{h}{(2^m\varepsilon + h)^2}. \quad (3.9)$$

The results of Corollary 3.1.2 may also be applied to the inverse of A_P, when an intermediate composite grid is used in place of the global coarse grid, by performing the replacement $m \leftarrow m - k$ $(0 \leqslant k < m)$.

In addition to these quantities, the pertinent quantities from the finite-volume discretization of [14, Chapter 4] are [here (u) denotes "upwind," and

(c), "centered"]:

$$
\begin{aligned}
l_{IC} &= -\varepsilon - h \text{ (u)}, & &-\varepsilon - h/2 \text{ (c)},\\
l_{CI} &= -\varepsilon \text{ (u)}, & &-\varepsilon + h/2 \text{ (c)},\\
r_{IC} &= -\varepsilon \text{ (u)}, & &-\varepsilon + h/2 \text{ (c)},\\
r_{CI} &= -\varepsilon - h \text{ (u)}, & &-\varepsilon - h/2 \text{ (c)},\\
l_{IF} &= -2^m\varepsilon \text{ (u)}, & &-2^m\varepsilon + h/2 \text{ (c)},\\
l_{FI} &= -2^m\varepsilon - h \text{ (u)}, & &-2^m\varepsilon - h/2 \text{ (c)},\\
r_{IF} &= -2^m\varepsilon - h \text{ (u)}, & &-2^m\varepsilon - h/2 \text{ (c)},\\
r_{FI} &= -2^m\varepsilon \text{ (u)}, & &-2^m\varepsilon + h/2 \text{ (c)},\\
l_{IP} &= -2^{m-k}\varepsilon \text{ (u)}, & &-2^{m-k}\varepsilon + h/2 \text{ (c)},\\
l_{PI} &= -2^{m-k}\varepsilon - h \text{ (u)}, & &-2^{m-k}\varepsilon - h/2 \text{ (c)},\\
r_{IP} &= -2^{m-k}\varepsilon - h \text{ (u)}, & &-2^{m-k}\varepsilon - h/2 \text{ (c)},\\
r_{PI} &= -2^{m-k}\varepsilon \text{ (u)}, & &-2^{m-k}\varepsilon + h/2 \text{ (c)},
\end{aligned}
$$

$$
L_I = \begin{bmatrix} (1+2^m)\varepsilon + h & 0 \\ 0 & (1+2^m)\varepsilon + h \end{bmatrix},
$$

$$
A_I = \begin{bmatrix} (1+2^{m-k})\varepsilon + h & 0 \\ 0 & (1+2^{m-k})\varepsilon + h \end{bmatrix} \text{(u)},
$$

$$
L_I = \begin{bmatrix} (1+2^m)\varepsilon & 0 \\ 0 & (1+2^m)\varepsilon \end{bmatrix},
$$

$$
A_I = \begin{bmatrix} (1+2^{m-k})\varepsilon & 0 \\ 0 & (1+2^{m-k})\varepsilon \end{bmatrix} \text{(c)}.
$$

Notice that we have allowed for general refinement on the coarse patch by letting $1 \leqslant k \leqslant m$. When $k = m$ this corresponds to letting the global coarse grid play the role of the coarse composite grid, and when $k = 1$ to using the grid having one less level of patch refinement than the true composite grid.

Now, using the above values along with the approximate values for the elements of the inverse matrices, we have for the U^4 case that

$$
\begin{aligned}
\hat{L}_I - \lambda\hat{A}_I = &\begin{bmatrix} (1+2^m)\varepsilon + h - \lambda[(1+2^{m-k})\varepsilon + h] & 0 \\ 0 & (1+2^m)\varepsilon + h - \lambda[(1+2^{m-k})\varepsilon + h] \end{bmatrix}\\
&+ (\lambda - 1)\begin{bmatrix} \varepsilon & 0 \\ 0 & \varepsilon \end{bmatrix} - \begin{bmatrix} 2^m\varepsilon & 0 \\ h & 2^m\varepsilon \end{bmatrix} + \lambda\begin{bmatrix} 2^{m-k}\varepsilon & 0 \\ h & 2^{m-k}\varepsilon \end{bmatrix}\\
&= L_I - \lambda A_I + (\lambda - 1)L_{IC}L_C^{-1}L_{CI} - L_{IF}L_F^{-1}L_{FI} + \lambda A_{IP}A_P^{-1}A_{PI}.
\end{aligned}
$$

A simple calculation then shows that irrespective of the value of k, the solutions of $\mathrm{Det}(\hat{L}_I - \lambda \hat{A}_I) = 0$ are $\lambda_1 = \lambda_2 = 1$.

Next, we consider the case where X represents a centered-difference discretization. Let

$$X = \mathrm{tri}\left[-\varepsilon - \frac{h}{2}, 2\varepsilon, -\varepsilon + \frac{h}{2}\right]$$

be of order N.

LEMMA 3.1.3. *The four corner elements of X^{-1} corresponding to the centered discretization are given by*

$$\tilde{x}_{11} = \tilde{x}_{NN} = \frac{(\varepsilon + h/2)^N - (\varepsilon - h/2)^N}{(\varepsilon + h/2)^{N+1} - (\varepsilon - h/2)^{N+1}} \approx \frac{1}{\varepsilon + h/2}, \tag{3.10}$$

$$\tilde{x}_{1N} = \frac{X_{N1}}{z_N} = \frac{h \cdot (-\varepsilon + h/2)^{N-1}}{(\varepsilon + h/2)^{N+1} - (\varepsilon - h/2)^{N+1}} \approx 0, \tag{3.11}$$

$$\tilde{x}_{N1} = \frac{X_{1N}}{z_N} = \frac{h \cdot (\varepsilon + h/2)^{N-1}}{(\varepsilon + h/2)^{N+1} - (\varepsilon - h/2)^{N+1}} \approx \frac{h}{(\varepsilon + h/2)^2}. \tag{3.12}$$

Proof. The jth determinant satisfies

$$z_j = -2\varepsilon z_{j-1} + \left(\varepsilon - \frac{h}{2}\right)\left(\varepsilon + \frac{h}{2}\right) z_{j-2}, \qquad j = 3, 4, \ldots, N,$$

with associated roots

$$\mu_1 = \varepsilon + \frac{h}{2}, \qquad \mu_2 = \varepsilon - \frac{h}{2}.$$

Hence,

$$z_j = S\left(\varepsilon + \frac{h}{2}\right)^j + T\left(\varepsilon - \frac{h}{2}\right)^j,$$

and in particular

$$z_1 = S\left(\varepsilon + \frac{h}{2}\right) + T\left(\varepsilon - \frac{h}{2}\right) = 2\varepsilon,$$

$$z_2 = S\left(\varepsilon + \frac{h}{2}\right)^2 + T\left(\varepsilon - \frac{h}{2}\right)^2 = 3\varepsilon^2 + \frac{h^2}{4}.$$

Solving for S and T, we find

$$S = \frac{\varepsilon + h/2}{h}, \qquad T = -\frac{\varepsilon - h/2}{h}.$$

Therefore,

$$z_j = \frac{(\varepsilon + h/2)^{j+1}}{h} - \frac{(\varepsilon - h/2)^{j+1}}{h},$$

and

$$\tilde{x}_{11} = \tilde{x}_{NN} = \frac{(\varepsilon + h/2)^N - (\varepsilon - h/2)^N}{(\varepsilon + h/2)^{N+1} - (\varepsilon - h/2)^{N+1}}.$$

Also,

$$\tilde{x}_{1N} = \frac{X_{N1}}{z_N} = \frac{h \cdot (-\varepsilon + h/2)^{N-1}}{(\varepsilon + h/2)^{N+1} - (\varepsilon - h/2)^{N+1}},$$

and

$$\tilde{x}_{N1} = \frac{X_{1N}}{z_N} = \frac{h \cdot (\varepsilon + h/2)^{N-1}}{(\varepsilon + h/2)^{N+1} - (\varepsilon - h/2)^{N+1}}. \qquad \blacksquare$$

In the discretization to be considered next, this approximation applies to A_P if the coarse patch has trivial refinement. For L_F we obtain the following corollary to Lemma 3.1.3.

COROLLARY 3.1.4. *The corner elements of the fine-patch matrix L_F corresponding to the centered discretization are given by*

$$\tilde{l}_{F_{11}} = \tilde{l}_{F_{N_F,N_F}} = \frac{\left(\varepsilon + h/2^{m+1}\right)^{N_F} - \left(\varepsilon - h/2^{m+1}\right)^{N_F}}{2^m\left[\left(\varepsilon + h/2^{m+1}\right)^{N_F+1} - \left(\varepsilon - h/2^{m+1}\right)^{N_F+1}\right]}$$

$$\approx \frac{1}{2^m\varepsilon + h/2}, \tag{3.13}$$

$$\tilde{l}_{F_{1,N_F}} = \frac{h\cdot\left(\varepsilon - h/2^{m+1}\right)^{N_F-1}}{2^{2m}\left[\left(\varepsilon + h/2^{m+1}\right)^{N_F+1} - \left(\varepsilon - h/2^{m+1}\right)^{N_F+1}\right]} \approx 0, \tag{3.14}$$

$$\tilde{l}_{F_{N_F,1}} = \frac{h\cdot\left(\varepsilon + h/2^{m+1}\right)^{N_F-1}}{2^{2m}\left[\left(\varepsilon + h/2^{m+1}\right)^{N_F+1} - \left(\varepsilon - h/2^{m+1}\right)^{N_F+1}\right]} \approx \frac{h}{\left(2^m\varepsilon + h/2\right)^2}. \tag{3.15}$$

A similar result holds for A_P when the coarse patch has nontrivial refinement, again by performing the replacement $m \leftarrow m - k$.

The next case we consider corresponds to the $(UC)^2$ discretization, which uses upwinding on the coarse component and centered on the patch for both the coarse and true composite grids. Using above approximations from the upwind and centered discretizations, we have

$$\hat{L}_I - \lambda\hat{A}_I = \begin{bmatrix} (1+2^m)\varepsilon + h - \lambda\left[(1+2^{m-k})\varepsilon + h\right] & 0 \\ 0 & (1+2^m)\varepsilon + h - \lambda\left[(1+2^{m-k})\varepsilon + h\right] \end{bmatrix}$$

$$+(\lambda-1)\begin{bmatrix} \varepsilon & 0 \\ 0 & \varepsilon \end{bmatrix} - \begin{bmatrix} 2^m\varepsilon & 0 \\ \dfrac{h(2^m\varepsilon + h)}{(2^m\varepsilon + h/2)} & \dfrac{(2^m\varepsilon - h/2)(2^m\varepsilon + h)}{2^m\varepsilon + h/2} \end{bmatrix}$$

$$+\lambda\begin{bmatrix} 2^{m-k}\varepsilon & 0 \\ \dfrac{h(2^{m-k}\varepsilon + h)}{(2^{m-k}\varepsilon + h/2)} & \dfrac{(2^{m-k}\varepsilon - h/2)(2^{m-k}\varepsilon + h)}{2^{m-k}\varepsilon + h/2} \end{bmatrix}.$$

The eigenvalues are $\lambda_1 = 1$ and

$$\lambda_2 = \frac{2^m\varepsilon + h}{2^m\varepsilon + h/2} \cdot \frac{2^{m-k}\varepsilon + h/2}{2^{m-k}\varepsilon + h} \in \left(\tfrac{1}{2}, 1\right] \qquad \text{for} \quad \varepsilon \in [0, \infty).$$

We consider briefly the validity of the approximations used here (a more thorough investigation of their validity appears in [14, Chapter 4]). On the one hand, we have used the approximate values in (3.4)–(3.6), which are valid with ε small with respect to h, for the coarse-component (upwind) operators. On the other hand, the (centered) approximations on the patch come from (3.10)–(3.12). Suppose that on the coarse composite grid no refinement is used on the patch ($m = 0$ and $N_F \leftarrow N_P$). Then the approximations will be valid with $\varepsilon \approx h/2$ and also if h continues to decrease. Notice that $\lambda_2 \to 1$ as $h \to 0$. Unfortunately, h approaching zero with ε fixed is at odds with the requirement for the coarse component. There are two approaches that avoid this predicament. The first approach is to use sufficient refinement on the coarse patch so that h need not be particularly small for (3.10)–(3.12) to be valid, because the exponent N_P (or N_F) appearing there increases with m. Also, notice that $\lambda_2 \approx 1$ with m large and k small (i.e., with sufficient refinement on the fine and coarse patches). Unfortunately, taking this approach rules out the use of the global coarse grid in the role of the coarse composite grid. The second approach allows for this possibility by altering the discretization on the coarse patch in order to weaken the requirement that h be small.

This leads us to consider the U^3C discretization, where upwinding is used throughout the coarse composite grid and on the coarse component of the composite grid, but centered differencing is used on the fine patch. As just observed, the following approximations will be valid with ε sufficiently small with respect to h (for the upwind approximation on the coarse component and on the coarse patch) and with sufficient refinement on the fine patch (for the centered approximation). Although our motivation here is to be able to use a coarse patch without refinement ($k = m$), we have carried out the analysis allowing arbitrary refinement on this region ($0 < k \leqslant m$). The eigenvalues are $\lambda_1 = 1$ and

$$\lambda_2 = \frac{2^m\varepsilon + h}{2^m\varepsilon + h/2},$$

which are independent of k. Notice that the desired effect has been achieved in that now λ_2 approaches unity while only requiring sufficient refinement on

the fine patch. The expressions for the eigenvalues are independent of the refinement used on the coarse patch, and so they will be valid, in particular, when the global coarse grid is used. We also remark that this requirement (of having sufficient refinement on the fine patch) is a natural one with respect to the use of the centered type of discretization for convection-dominated problems. Although the expression for λ_2 is only valid in certain parameter ranges of the one-dimensional problem, we will see that the quantity $\lambda_2 - 1$ supplies a fairly accurate approximation to the actual convergence factor even in two dimensions.

Collecting the results from our examination of the various cases considered above establishes the following theorem and corollary which apply to the one-dimensional problem.

THEOREM 3.1.5. *Suppose that the exact values of the corner elements in equations* (3.4)–(3.15) *are replaced by their corresponding approximations. Then, in the* U^4 *case, and as* $m \to \infty$ *in the* U^3C *case, we have the following.*

Both eigenvalues of $I - \hat{L}_I \hat{A}_I^{-1}$ *are zero. Therefore, two steps of the iteration*

$$\mathbf{r}_I^{i+1} = \left(I - \hat{L}_I \hat{A}_I^{-1}\right)\mathbf{r}_I^i$$

drive the residual at the interface to zero. This matrix is in fact strictly lower triangular: the "left" and "right" components of the interface residual vanish in the first and second steps, respectively, of the iteration.

COROLLARY 3.1.6. *Suppose the two-level FAC scheme is written in the form* $\underline{\mathbf{r}}^{i+1} = (\underline{\boldsymbol{I}} - \underline{\boldsymbol{L}}\underline{\boldsymbol{M}}^{-1})\underline{\mathbf{r}}^i$ *for some composite preconditioner* $\underline{\boldsymbol{M}}$. *Then, with the assumptions of Theorem* 3.1.5, *this iteration matrix is nilpotent:* $(\underline{\boldsymbol{I}} - \underline{\boldsymbol{L}}\underline{\boldsymbol{M}}^{-1})^3 = 0$, *i.e., the two-level scheme converges in three iterations and thus may be considered a direct method.*

Proof. The corollary follows from the vanishing of $\mathbf{r}_C^i$ and $\mathbf{r}_F^i$ established in [14] for $i \geqslant 1$, the resulting expression (3.2) for the updating of the interface component of the residual, and Theorem 3.1.5.

It should be noted that the results of the last theorem (and its corollary) are largely independent of the choice of coarse composite grid, i.e., they hold with $m - k$ levels of refinement on the coarse patch for all values of k, $0 \leqslant k \leqslant m$. In particular, this motivates the use of the global coarse grid in

this capacity. An extension of these results to the case of multiple regions of refinement is given in [14].

3.2. *Convergence in Two Dimensions*

In this section we study the convergence of two-level FAC applied to the solution of the finite-volume discretization of the problem (1.4). The examination here is experimental in nature. Guided by the results of the previous section, we attempt to determine to what extent the results for the one-dimensional problem carry over to two dimensions. Motivated by the findings of that section, we concentrate our study on the behavior of an algorithm that emphasizes the use of the global coarse grid. The numerical method used here to solve the composite-grid equations is the two-level FAC scheme with the global coarse grid at the coarse level. Subproblems (corresponding to the fine patch and global coarse systems) are solved "exactly" (i.e., iteratively with a tolerance on the relative residual of 10^{-6}). This has been done by performing, in the appropriate context, the necessary number of relaxations or multigrid V-cycles (for further details see [14, §5.3.1]).

The first result emphasizes the effect that the initial guess has on the convergence behavior. We consider the solution of the upwind/upwind discretization of (1.4) with $\varepsilon = 10^{-4}$. The composite grid has coarse-component meshwidth $h = \frac{1}{32}$ and $m = 4$ levels of patch refinement. A 9×11 interface having its southwest corner at the (lexicographically ordered) coarse-component node (13, 8) is used. The right-hand side for (1.4) is that of Problem 3.1 in [14, §3.3.1]. The upwind/upwind discretization is also used on the global coarse grid (in the role of the coarse composite grid). This corresponds to use of the U^4 technique as described in the previous section. Table 1 presents the sequences of relative composite residuals corresponding to two solutions of the discrete problem. The two solves differ in the choice of the initial composite guess $\underline{z}^0$. The zero vector and a random vector with elements between zero and one were used. The results appear, respectively, in the left and middle columns of the table. Recall that $\|\underline{r}^i\|_2$ here actually measures the current interface component of the residual, since $r_C^i, r_F^i = 0$ for $i \geqslant 1$ (see Section 3.1). Notice that there is a significant difference in the rates at which these interface residuals approach zero in the two solves. This difference is due to the convergence behavior of the residuals at the nodes that correspond to the tangential (north and south) boundaries of the interface. At the in- and outflow (west and east, respectively) boundaries, the convergence behavior is like that predicted by the analysis of the one-dimensional problem—in both solves the residuals at the interface converge rapidly to zero. However, at the tangential boundaries the convergence rate is generally much slower, as in the middle column of Table 1. The reason that

TABLE 1
RELATIVE RESIDUALS AS FUNCTIONS OF FAC ITERATIONS USING THE U^4 METHOD IN TWO DIMENSIONS[a]

	$\|\underline{\mathbf{r}}^i\|_2/\|\underline{\mathbf{r}}^0\|_2$		
i	$\underline{\mathbf{z}}^0 = 0$	$\underline{\mathbf{z}}^0$ random	Modified stencil, $\underline{\mathbf{z}}^0$ random
1	1.825×10^{-4}	6.406×10^{-2}	5.592×10^{-2}
2	3.355×10^{-6}	1.411×10^{-2}	1.108×10^{-3}
3	6.803×10^{-7}	6.208×10^{-3}	9.313×10^{-5}
4	—	2.742×10^{-3}	8.291×10^{-6}
5	—	1.212×10^{-3}	6.013×10^{-7}
6	—	5.358×10^{-4}	—
7	—	2.370×10^{-4}	—
8	—	1.049×10^{-4}	—
9	—	4.639×10^{-5}	—
10	—	2.053×10^{-5}	—

[a]Composite grid, upwind/upwind.

this effect does not appear initially in the left column is that, with the initial guess of zero, very accurate solution values are produced at the tangential boundaries as a result of the first global coarse solve. Thus, the residuals at these nodes are extemely small at the end of the first FAC iteration and therefore throughout the ensuing iterations.

We have developed a remedy for the problem of slow convergence at the tangential boundaries that involves modifying the definition of the global coarse stencil at these nodes. The right column of Table 1 gives the results for a solve using this modification. The actual changes to the stencil are obtained by requiring that interface-to-interface connections for the global coarse operator agree with those of the composite operator, i.e., $A_I = L_I$ at nodes lying on the tangential boundaries. As a practical matter, these changes do not adversely affect the efficiency of the algorithm's implementation. On the contrary, they can be beneficial, making the global coarse matrix more diagonally dominant, which facilitates the solution of these equations by an iterative method.

To motivate these modifications, consider the case where the only interface component is a tangential one, i.e., the two-dimensional composite grid associated with the domain partitioned into two horizontal strips, as depicted in Figure 3. Also, let $\varepsilon \to 0$. Then, since all the vertical connections of the matrix stencils (see [14, §3.2.3]) are zero, it follows that the composite operator $\underline{\boldsymbol{L}}$ in (3.1) is strictly block diagonal. The same is true for $\underline{\mathbf{A}}$. The Schur complements of these respective operators then become L_I and A_I,

and the equation for the updating of the interface residual simplifies to

$$\mathbf{r}_I^{i+1} = \left(I_I - L_I A_I^{-1}\right)\mathbf{r}_I^i.$$

This clarifies the reason for the modification. We note that without the modification, $A_I = (1/s)L_I$, where $s = \frac{1}{2} + 1/2^{m+1}$. Thus

$$\mathbf{r}_I^{i+1} = (1 - s)\mathbf{r}_I^i,$$

giving convergence factors between one-quarter and one-half. This agrees roughly with the observed convergence rates. We remark that as $\varepsilon \to 1$ the modification becomes less beneficial, and even detrimental, but the way that this happens depends on both ε and the amount of patch refinement.

Tables 2–3 show convergence rates as functions of ε and fine-patch refinement for the U^4 method applied to the upwind/upwind discretization of this problem. The coarse-component meshwidth is $h_C = \frac{1}{32}$, and m gives the number of additional levels of refinement on the fine patch. We used a random initial guess throughout in these tests and, in some cases, the modification to the global coarse stencil mentioned above. We found that the advantage gained by using this modification is lost as ε increases, and use of the unmodified stencil can give better performance. For a given ε, the results appearing in Tables 2–3 correspond to whichever strategy showed

TABLE 2

FAC CONVERGENCE AS A FUNCTION OF ε FOR THE U^4 METHOD[a]

	$\|\mathbf{r}^i\|_2/\|\mathbf{r}^0\|_2$			
	Unmodified stencil,	Modified stencil		
i	$\varepsilon = 10^{-2}$	$\varepsilon = 10^{-3}$	$\varepsilon = 10^{-4}$	$\varepsilon = 10^{-5}$
1	5.964×10^{-2}	6.824×10^{-2}	8.160×10^{-2}	8.403×10^{-2}
2	4.287×10^{-3}	5.606×10^{-4}	1.654×10^{-4}	2.071×10^{-5}
3	4.554×10^{-4}	1.737×10^{-5}	4.138×10^{-7}	1.790×10^{-7}
4	5.855×10^{-5}	8.934×10^{-7}	—	—
5	8.080×10^{-6}	—	—	—
6	1.143×10^{-6}	—	—	—
7	2.269×10^{-7}	—	—	—
8	—	—	—	—
9	—	—	—	—
10	—	—	—	—

[a]Composite grid, upwind/upwind, $m = 1$.

TABLE 3
FAC CONVERGENCE AS A FUNCTION OF ε FOR THE U^4 METHOD[a]

	$\|\underline{r}^i\|_2/\|\underline{r}^0\|_2$			
	Unmodified stencil		Modified stencil	
i	$\varepsilon = 10^{-2}$	$\varepsilon = 10^{-3}$	$\varepsilon = 10^{-4}$	$\varepsilon = 10^{-5}$
1	1.691×10^{-1}	7.516×10^{-2}	5.592×10^{-2}	5.738×10^{-2}
2	1.232×10^{-2}	1.506×10^{-2}	1.108×10^{-3}	4.108×10^{-5}
3	1.135×10^{-3}	3.523×10^{-3}	9.313×10^{-5}	4.659×10^{-7}
4	1.192×10^{-4}	1.171×10^{-3}	8.291×10^{-6}	—
5	1.259×10^{-5}	4.012×10^{-4}	6.013×10^{-7}	—
6	1.321×10^{-6}	1.384×10^{-4}	—	—
7	2.078×10^{-7}	4.786×10^{-5}	—	—
8	—	1.657×10^{-5}	—	—
9	—	5.769×10^{-6}	—	—
10	—	2.014×10^{-6}	—	—

[a]Composite grid, upwind/upwind, $m = 4$.

better performance. Thus, the leftmost column of Table 2 and the two leftmost columns of Table 3 correspond to the use of the unmodified stencil, while the other results are for the modified stencil. Notice that the convergence rates generally improve as ε decreases, which is what we would expect as a result of the analysis of Section 3.1. The analysis also predicts nonindependence of the rates on the level of patch refinement. The results here show a mild degradation as the level of refinement is increased. One possible way to offset this effect (i.e., to make the need for refinement less critical) is to use a more accurate upwind scheme on the fine patch.

Table 4 shows results of a similar set of experiments with standard upwinding replaced by higher-order upwinding (Hup) [14] on the fine patch, i.e., the $(UH)^2$ technique (here, H denotes the use of the higher-order upwind discretization on a composite grid component) is used to solve the upwind/ Hup composite grid problem. These experiments indicate that its convergence behavior strongly resembles that of U^4 (compare Tables 4 and 3 —the same strategy as above, of modifying the interface stencil, has been used here). When combined with a comparison of the accuracy of the two upwind discretizations (see [14, Chapter 3]), these and other similar results indicate that there is little advantage to using the upwind/upwind discretization. The more accurate upwind/Hup method can be used without sacrificing efficiency. In our implementation of FAC for the problem (1.4) we used strategies based on block Jacobi relaxation to solve the patch systems. With the upwind discretization, this means performing back substitutions associ-

TABLE 4
FAC CONVERGENCE AS A FUNCTION OF ε FOR THE $(UH)^2$ METHOD[a]

	$\|\underline{r}^i\|_2/\|\underline{r}^0\|_2$			
	Unmodified stencil		Modified stencil	
i	$\varepsilon = 10^{-2}$	$\varepsilon = 10^{-3}$	$\varepsilon = 10^{-4}$	$\varepsilon = 10^{-5}$
1	1.674×10^{-1}	7.082×10^{-2}	4.933×10^{-2}	5.026×10^{-2}
2	1.389×10^{-2}	1.352×10^{-2}	1.158×10^{-3}	7.143×10^{-5}
3	1.286×10^{-3}	3.247×10^{-3}	8.733×10^{-5}	3.364×10^{-7}
4	1.368×10^{-4}	1.086×10^{-3}	7.515×10^{-6}	—
5	1.487×10^{-5}	3.718×10^{-4}	5.304×10^{-7}	—
6	1.643×10^{-6}	1.281×10^{-4}	—	—
7	2.377×10^{-7}	4.424×10^{-5}	—	—
8	—	1.531×10^{-5}	—	—
9	—	5.326×10^{-6}	—	—
10	—	1.852×10^{-6}	—	—

[a]Composite grid, upwind/Hup, $m = 4$.

ated with the inversion of tridiagonal blocks at each relaxation step. With the more accurate method, the increase in work corresponds to using blocks having one additional diagonal.

We present results in Table 5 for the U^3C method applied to the upwind/centered discretization with various ε and m. The convergence rates improve as $\varepsilon \cdot 2^m$ increases, as predicted by the analysis of the previous

TABLE 5
FAC CONVERGENCE AS A FUNCTION OF ε AND m FOR THE U^3C METHOD[a]

	$\|\underline{r}^i\|_2/\|\underline{r}^0\|_2$			
	$m = 1$		$m = 4$	
i	$\varepsilon = 10^{-2}$	$\varepsilon = 10^{-3}$	$\varepsilon = 10^{-2}$	$\varepsilon = 10^{-3}$
1	6.790×10^{-2}	1.149×10^{-1}	1.784×10^{-1}	1.011×10^{-1}
2	1.243×10^{-2}	8.888×10^{-2}	1.577×10^{-2}	3.178×10^{-2}
3	4.134×10^{-3}	7.106×10^{-2}	1.512×10^{-3}	1.343×10^{-2}
4	1.515×10^{-3}	5.875×10^{-2}	1.627×10^{-4}	5.692×10^{-3}
5	5.744×10^{-4}	4.978×10^{-2}	1.782×10^{-5}	2.489×10^{-3}
6	2.223×10^{-4}	4.298×10^{-2}	2.008×10^{-6}	1.103×10^{-3}
7	8.735×10^{-5}	3.759×10^{-2}	2.787×10^{-7}	4.958×10^{-4}
8	3.470×10^{-5}	3.318×10^{-2}	—	2.253×10^{-4}

[a]Composite grid, upwind/centered.

section. We note, however, a limit to the applicability of this result in that ε must not be allowed to become too large. If ε is allowed to increase with h and m fixed, a degradation of the convergence rates occurs. This fact is in accordance with the requirement, in the analysis of this method, that ε remain small enough to ensure the validity of the approximations used with respect to the upwind stencil on the coarse components.

Finally, in Table 6 we compare predicted convergence factors for the U^3C method, namely the quantity $1 - \lambda_2$ of Section 3.1, with the average rates, $\|\underline{\mathbf{r}}^i\|/\|\underline{\mathbf{r}}^0\|^{1/i}$ corresponding to the results in Table 5. Here, the value of i corresponds to the final iterate in a given column of that table. We see that the approximations give reasonable (although generally somewhat pessimistic) estimates of actual convergence rates.

4. SUMMARY OF RESULTS

In this paper, we have studied FAC convergence for convection-dominated elliptic equations in one and two dimensions. We concentrated on problems using significant local refinement on a composite grid. Although the results obtained for the one-dimensional case are generally of little practical interest in themselves, they provide important insight into the behavior of the methods we study in two dimensions.

In two dimensions, the results of this study were obtained for the equation

$$-\varepsilon\Delta u + u_x + cu = f. \tag{4.1}$$

This equation has a particularly attractive form in that its flow velocity lies entirely in the x-coordinate direction. We noted that this equation can be

TABLE 6
COMPARISON OF ACTUAL AND PREDICTED CONVERGENCE FACTORS FOR THE U^3C METHOD

	$m = 1$		$m = 4$	
	$\varepsilon = 10^{-2}$	$\varepsilon = 10^{-3}$	$\varepsilon = 10^{-2}$	$\varepsilon = 10^{-3}$
$\lvert 1 - \lambda_2 \rvert$[a]	2.77×10^{-1}	6.53×10^{-1}	1.16×10^{-1}	3.50×10^{-1}
$(\|\underline{\mathbf{r}}^i\|_2/\|\underline{\mathbf{r}}^0\|_2)^{1/i}$	4.39×10^{-1}	8.87×10^{-1}	8.90×10^{-2}	4.94×10^{-1}

[a] $\lambda_2 = (2^m\varepsilon + h)/(2^m\varepsilon + h/2)$.

obtained from a rather general convection-diffusion equation in two dimensions via a change of coordinates based on the characteristics. Algorithms for performing this change of coordinates are described in [4] and [5].

The significance of the above form for the results obtained herein are twofold, corresponding to two hierarchies of solution procedure. At the global level, we considered the FAC method for the solution of (4.1) discretized on a composite grid. This method places the computational effort in solving (or ultimately, partially solving) standard problems on subregions of the composite grid. Our convergence results for this method relied, to a large extent, on the strong one-dimensional character of (4.1) when ε is small, in the sense that when this is true a rigorous analysis in one dimension gives much useful insight into the true behavior of FAC convergence in two dimensions.

In Section 3.1 we analyzed the eigenvalues of what is essentially the iteration matrix governing convergence of two-level FAC when applied to the one-dimensional version of (4.1). Three discretizations of this problem were considered, which involved varying discretization types on the components and levels of the grid. The first case (the U^4 method) involved the use of upwind discretization throughout both grids. In suitable parameter ranges, we concluded that the spectral radius of the iteration matrix, in this case, was zero. This allowed us to further conclude that in this context the two-level FAC iteration may be viewed as a direct solver, producing a zero residual after three iterations. Furthermore, this result was relatively insensitive to the choice of the composite grid used on the coarse level. In particular, the global coarse grid may be used. The second case we considered, $(UC)^2$ used upwind and centered-difference discretizations, respectively, on the coarse component and the patch component of the two grids. The spectral radius of the iteration matrix in this case was bounded by one-half, but the validity of the result depended on a familiar requirement for the centered discretization, namely that the meshwidth h be sufficiently small with respect to the diffusion coefficient. This was in conflict with the requirement for the upwind part of the discretization and motivated the use of the third strategy, U^3C, which employed upwinding throughout the coarse grid and used the upwind/centered mix on the composite grid. For this case, the spectral radius approached zero as the refinement level on the fine patch increased.

As for convergence in two dimensions, we saw in Section 3.2 that computational results conformed generally to the analysis in one dimension. This was particularly true for the U^3C method. In fact, we saw that for this method the predicted convergence factors of Section 3.1 provided accurate approximations to empirical convergence factors in two dimensions (recall Tables 5–6). This information can be useful in determining *a priori* when to employ the centered discretization on the fine patch, depending on the number of levels of refinement used. It can also be used as a criterion for

switching discretization types when FAC is used in a nested fashion on a sequence of composite grids.

An exception to the behavior predicted by the analysis of Section 3.1 was a significant degradation in convergence rates with upwinding used on the fine patch when the diffusion coefficient was small. We found that this was caused by slow convergence of the residuals at the tangential boundaries of the patch (i.e., the ones parallel to the flow direction). By analyzing the matrix stencil associated with an idealized version of the problem (the case that the interface component is all tangential boundary), we identified a modification of the stencil in these regions that restores the convergence rates. The modification had essentially the same effect when higher-order upwinding was used on the fine patch. In fact, in our experience, results obtained for standard upwinding generally apply as well to the use of higher-order upwinding. These include global convergence behavior of two-level FAC as well as weighting of line relaxation in devising multigrid smoothers for subgrid problems.

We note that if the two-level schemes U^4 and U^3H of Section 3 are used as iterative solvers (i.e., viewed as preconditioned iterations and accelerated by a polynomial method) and ε is small, it is essential that the modification to the coarse-grid stencil described there be performed. Just how small ε must be for this to be necessary depends on the meshwidth of both the coarse and fine components of the composite grid. In our experiments, with the coarse meshwidth fixed this point occurred later (with respect to decreasing ε) as the number of levels of fine patch refinement increased (see Tables 2–3).

However, we do not advocate such use in general. The reason for this is that the two-level scheme, as presented in Section 3, requires exact solution of the (global coarse- and fine-patch) subgrid problems. Furthermore, as noted in [10], with respect to diffusion problems, the number of iterations required to solve the composite equations grows rapidly when a few steps of a multigrid method are used to approximately solve the fine-patch subproblems. Therefore, the computational complexity of the two-level scheme is generally far from optimal. Yet, there is a way of combining the scheme with efficient approximation of subgrid solutions which does have the (fine-grid) complexity of full multigrid. The approach we find more appealing is the classical multigrid approach of using the scheme in a nested way on a sequence of successively finer grids. A description of such a method and recommendations for its implementation may be found in [14]. There, we use the two-level scheme as a weak algebraic solver on each of the composite grids lying between the global coarse grid and the true composite grid, and use inexpensive subproblem approximations obtained via either relaxation or multigrid V-cycles. Computational results in [14] show that, for the various discretization mixtures, only one or two FAC iterations are required on each

of the composite levels to obtain an approximation by this version of FAC with accuracy comparable to the exact solution of the composite-grid equations. Furthermore, it is shown that this is the case with complete solves of subgrid problems replaced by inexpensive approximations. This is significant because practitioners of the two-level approach have noted dramatic degradation in global convergence when subproblems on the fine patch are solved approximately (see [10], for example). The above method, however, yields accurate solutions with optimal efficiency on this region, i.e., the total amount of work there is comparable to that of a classical full multigrid iteration [3].

I would like to thank Tom Manteuffel and Steve McCormick for motivating this work, for providing guidance and editorial input, and for their support, advice, and encouragement during the preparation of my doctoral thesis from which this material is taken.

REFERENCES

1 R. Bank and M. Benbourenane, A Fourier analysis of the two-level hierarchical basis multigrid method for convection-diffusion equations, in *Proceedings of the Fourth International Conference on Domain Decomposition Methods for Partial Differential Equations* (R. Glowinski, Y. A. Kuznetsov, G. Meurant, J. Périaux, and O. B. Widlund, Eds.), SIAM, Philadelphia, 1991, pp. 178–184.

2 J. H. Bramble, R. E. Ewing, J. E. Pasciak, and A. H. Schatz, A preconditioning technique for the efficient solution of problems with local grid refinement, *Comput. Methods Appl. Mech. Engrg.* 67:149–159 (1988).

3 W. L. Briggs, *A Multigrid Tutorial*, SIAM, Philadelphia, 1987.

4 D. L. Brown, R. C. Y. Chin, G. W. Hedstrom, and T. A. Manteuffel, Layer Tracking, Asymptotics and Domain Decomposition, Technical Report UCRL-JC-106336, Lawrence Livermore National Lab., 1991.

5 R. C. Y. Chin, G. W. Hedstrom, F. A. Howes, and J. R. McGraw, Parallel computation of multiple-scale problems, in *New Computing Environments: Parallel, Vector and Systolic* (A. Wouk, Ed.), SIAM, Philadelphia, 1986.

6 R. C. Y. Chin and T. A. Manteuffel, An analysis of block successive overrelaxation for a class of matrices with complex spectra, *SIAM J. Numer. Anal.* 25:564–585 (1988).

7 R. W. Cottle, Manifestations of the Schur complement, *Linear Algebra Appl.*, 8:189–211 (1974).

8 R. E. Ewing, Domain decomposition techniques for efficient adaptive local grid refinement, in *Proceedings of the Second International Symposium on Domain Decomposition Methods* (T. F. Chan, R. Glowinski, J. Périaux, and O. B. Widlund, Eds.), SIAM, Philadelphia, 1989, pp. 192–206.

9 R. E. Ewing, R. D. Lazarov, and P. S. Vassilevski, Local refinement techniques for elliptic problems on cell-centered grids, I: error estimates, *Math. Comp.* 56:437–461 (1991).

10 R. E. Ewing, R. D. Lazarov, and P. S. Vassilevski, Local refinement techniques for elliptic problems on cell-centered grids, II: Optimal order two-grid iterative methods, submitted for publication.
11 W. Hackbusch, Multigrid convergence for a singular perturbation problem, *Linear Algebra Appl.*, 58:125–145 (1984).
12 S. F. McCormick, Fast adaptive composite grid (FAC) methods: Theory for the variational case, in *Defect Correction Methods: Theory and Applications* (K. Böhmer and H. J. Stetter, Eds.), Comput. Suppl. 5, Springer-Verlag, Wien, 1984, pp. 115–122.
13 S. F. McCormick, *Multilevel Adaptive Methods for Partial Differential Equations*, Frontiers Appl. Math. 6, SIAM, Philadelphia, 1989.
14 J. S. Otto, Multilevel Methods for the Solution of Advection-Dominated Elliptic Problems on Composite Grids, Doctoral Thesis, Dept. of Mathematics, Univ. of Colorado at Denver, 1992.
15 P. J. Roach, *Computational Fluid Dynamics*, Hermosa, Albuquerque, 1972.
16 O. B. Widlund, Optimal Iterative Refinement Methods, Technical Report 391, Dept. of Computer Science, Courant Inst. of Mathematical Sciences, New York, 1988.

Received 16 April 1992; final manuscript accepted 28 August 1992